Contribution from the School of Chemical Sciences, University of Illinois, Urbana, Illinois 61801, Department of Chemistry, Columbia University, New York, New York 10027, Crystalytics Company, Lincoln, Nebraska 68501, and Department of Chemistry, University of Nebraska, Lincoln, Nebraska 68588

Synthesis and Structure of the $[(OC)_3Mn(cis\text{-}Nb_2W_4O_{19})]^{3-}$ and $[(OC)_3Re(cis\text{-}Nb_2W_4O_{19})]^{3-}$ Anions

C. J. BESECKER,[1a] V. W. DAY,*[1b,c] W. G. KLEMPERER,*[1a] and M. R. THOMPSON[1c]

Received May 1, 1984

Reaction of $(cis\text{-}Nb_2W_4O_{19})[(n\text{-}C_4H_9)_4N]_4$ with $[fac\text{-}(OC)_3M(NCCH_3)_3]X$ (M = Mn, X = Br; M = Re, X = PF_6) in CH_3CN yields $[(OC)_3M(Nb_2W_4O_{19})]^{3-}$ [M = Mn (**1**), Re (**2**)] as $(n\text{-}C_4H_9)_4N^+$ salts. Anions **1** and **2** are isostructural according to infrared spectroscopy, and a single-crystal X-ray diffraction study of the manganese salt reveals a structure in which a disordered $Nb_2W_4O_{19}^{4-}$ ligand is coordinated to a metal tricarbonyl unit by a triangle of three adjacent bridging oxygens. Three diastereomers are possible for this structure. In isomer I, the $M(CO)_3$ binding site is formed by an ONb_2 oxygen plus two ONbW oxygens. Two ONbW oxygens plus an OW_2 oxygen are involved in isomer II, and three OW_2 oxygens form the binding site in isomer III. Oxygen-17 NMR spectra show that diastereomer II predominates in solutions of **1** and **2** but that diastereomers I and III are also present at lower concentrations.

Introduction

The chemistries of both low-valent transition-metal organometallics and high-valent transition-metal polyoxoanions have been studied in great detail, but very little attention has been focused on interactions between complexes in these two families.[2-5] Many transition-metal polyoxoanions have rigid structures based on extended close-packed oxygen arrays. They are therefore able to provide reactive organometallic units with a variety of geometrically well-defined binding sites that are conformationally inflexible well beyond the first coordination sphere of the organometallic center. The objective of the present study was the exploration of this potential through the isolation of stable adducts of low-valent transition-metal organometallics and high-valent transition-metal polyoxoanions that are amenable to detailed physical and structural characterization.[6] The successful preparation and characterization of stable adducts would set the stage for systematic investigation of more reactive analogues.

The $cis\text{-}Nb_2W_4O_{19}^{4-}$ ion[7-10] was selected as a prototypical polyoxoanion ligand for several reasons. It has a rigid, C_{2v} structure shown in a consisting of three cubic close-packed layers

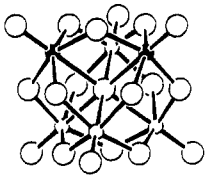

a

of oxygen atoms linked by six d^0 metal centers, arranged in a cis-octahedral fashion, which occupy octahedral interstices between these layers. If idealized to an M_6O_{19} framework, the structure has O_h symmetry and presents eight equivalent planar oxygen surfaces, each containing a central triangle of three bridging oxygens and a peripheral triangle of three terminal oxygens. Although the $W_6O_{19}^{2-}$ anion[11-13] has this highly symmetric structure, it was not suitable for the present investigation due to insufficient nucleophilicity arising, presumably, from low surface charge. The more highly charged, more nucleophilic $cis\text{-}Nb_2W_4O_{19}^{4-}$ ion was chosen in preference to the isostructural $cis\text{-}V_2W_4O_{19}^{4-}$ ion[14,15] in order to avoid redox chemistry that might result from reaction of a low-valent organometallic with the strongly oxidizing V^V centers. A final factor taken into consideration was the ability to prepare the $Nb_2W_4O_{19}^{4-}$ ion on a large scale in high yield as a $(n\text{-}C_4H_9)_4N^+$ salt[10] which has high solubility in several aprotic solvents suitable for organometallic reaction chemistry.

The choice of the $fac\text{-}(OC)_3Mn(NCCH_3)_3^+$ and $fac\text{-}(OC)_3Re(NCCH_3)_3^+$ cations[16-18] as organometallic starting materials was also dictated by several considerations. As cations, these organometallic units should be predisposed to react with polyoxoanions on electrostatic grounds alone. They have been shown to react readily with several different two-electron donor ligands L to form kinetically stable d^6 low-spin octahedral 18-electron complexes $fac\text{-}(OC)_3ML_3^+$ (M = Mn, Re)[16-18] and might form analogous complexes with $Nb_2W_4O_{19}^{4-}$ where L_3 represents a triangle of adjacent surface oxygens. Should these oxygens all be bridging oxygens in the $Nb_2W_4O_{19}^{4-}$ structure, the metal tricarbonyl unit would occupy a conformationally rigid binding site of the type referred to above.

In a preliminary paper,[3] we described the preparation of $[(OC)_3Mn(Nb_2W_4O_{19})]^{3-}$ and $[(OC)_3Re(Nb_2W_4O_{19})]^{3-}$ as $(n\text{-}C_4H_9)_4N^+$ salts and their structural characterization using IR and 13.5-MHz ^{17}O NMR techniques. We report here a more detailed investigation that includes single-crystal X-ray diffraction and 33.9-MHz ^{17}O NMR studies.

Experimental Section

Reagents, Solvents, and General Procedures. The following were purchased from commercial sources and used without further purification: $Mn_2(CO)_{10}$, $Re_2(CO)_{10}$, and $AgPF_6$ (Strem); Br_2 (Fisher); $^{17}OH_2$ (Monsanto Research).

(1) (a) University of Illinois (current address) and Columbia University. (b) Crystalytics Co. (c) University of Nebraska.
(2) Knoth, W. H. *J. Am. Chem. Soc.* **1979**, *101*, 2211-3.
(3) Besecker, C. J.; Klemperer, W. G. *J. Am. Chem. Soc.* **1980**, *102*, 7598-600. The ^{17}O NMR spectra reported here show no carbonyl resonances on account of insufficient ^{17}O enrichment resulting from mild preparative conditions.
(4) Day, V. W.; Fredrich, M. F.; Thompson, M. R.; Klemperer, W. G.; Liu, R.-S.; Shum, W. *J. Am. Chem. Soc.* **1981**, *103*, 3597-9.
(5) Besecker, C. J.; Klemperer, W. G.; Day, V. W. *J. Am. Chem. Soc.* **1982**, *104*, 6158-9.
(6) See ref 3 for a preliminary report of this work.
(7) Dabbabi, M.; Boyer, M. *J. Inorg. Nucl. Chem.* **1976**, *38*, 1101-4.
(8) Rocchiccioli-Deltcheff, C.; Thouvenot, R.; Dabbabi, M. *Spectrocnim. Acta, Part A* **1977**, *33A*, 143-54.
(9) Dabbabi, M.; Boyer, M.; Launay, J.-P.; Jeannin, Y. *J. Electroanal. Chem.* **1977**, *76*, 153-64.
(10) Besecker, C. J.; Day, V. W.; Klemperer, W. G.; Thompson, M. R., *J. Am. Chem. Soc.* **1984**, *106*, 4125-36.
(11) Jahr, K. R.; Fuchs, J.; Oberhauser, R. *Chem. Ber.* **1968**, *101*, 477-81.
(12) Henning, G.; Hüllen, A. *Z. Kristallogr.* **1969**, *130*, 162-72.
(13) Fuchs, J.; Freiwald, W.; Hartl, H. *Acta Crystallogr., Sect. B: Struct. Crystallogr. Cryst. Chem.* **1978**, *B34*, 1764-70.
(14) Nishikawa, K.; Kobayashi, A.; Sasaki, Y. *Bull. Chem. Soc. Jpn.* **1975**, *48*, 889-92 and references cited therein.
(15) Klemperer, W. G.; Shum, W. *J. Am. Chem. Soc.* **1978**, *100*, 4891-3.
(16) Reimann, R. H.; Singleton, E. *J. Organomet. Chem.* **1973**, *59*, C24-6.
(17) Reimann, R. H.; Singleton, E. *J. Chem. Soc., Dalton Trans.* **1974**, 808-13.
(18) Edwards, D. A.; Marshalsea, J. *J. Organomet. Chem.* **1977**, *131*, 73-91.

0020-1669/85/1324-0044$01.50/0

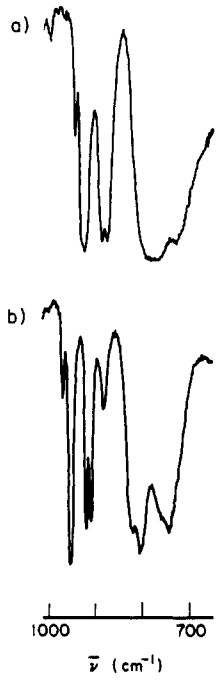

Figure 1. IR spectra of (a) $(Nb_2W_4O_{19})[(n\text{-}C_4H_9)_4N]_4$ and (b) $[(OC)_3Mn(Nb_2W_4O_{19})][(n\text{-}C_4H_9)_4N]_3$ measured from Nujol mulls. The infrared spectrum of $[(OC)_3Re(Nb_2W_4O_{19})][(n\text{-}C_4H_9)_4N]_3$, except for small differences in wavenumber values, is virtually indistinguishable from the spectrum shown in (b). See Experimental Section for numerical data.

$Mn(CO)_5Br$,[19] $Re(CO)_5Br$,[19] and $(Nb_2W_4O_{19})[(n\text{-}C_4H_9)_4N]_4$[10] were prepared according to literature procedures. $[(OC)_3Re(NCCH_3)_3]PF_6$ was prepared according to the procedure reported for the analogous ClO_4^- salt[18] using $AgPF_6$ instead of $AgClO_4$. Oxygen-17 enrichment of $(Nb_2W_4O_{19})[(n\text{-}C_4H_9)_4N]_4$ was accomplished by using the method described in ref 10. This material was used to prepare ^{17}O-enriched $Mn(CO)_3^+$ and $Re(CO)_3^+$ adducts following the preparative procedures given below.

Anhydrous diethyl ether (Mallinckrodt) was used only from freshly opened cans. Acetonitrile (Aldrich, 99%) and dichloromethane (Fisher) were distilled under N_2 from P_4O_{10} onto activated 3-Å molecular sieves. Toluene and carbon tetrachloride (both Fisher) were stored over activated 4-Å molecular sieves. Solvents used for the preparation of ^{17}O-enriched samples were purified more thoroughly and used within 48 h after distillation. Toluene was distilled under N_2 from sodium benzophenone ketyl. Prepurified acetonitrile and dichloromethane were distilled under N_2 from CaH_2. The middle fractions were collected and stored over activated 3-Å molecular sieves. Molecular sieves were activated by drying at 350 °C for 24 h and storing under N_2 at room temperature.

Reactions involving manganese and rhenium reagents were routinely performed in an N_2 atmosphere. All manipulations of ^{17}O-enriched materials were performed in closed systems with rigorous exclusion of atmospheric moisture to avoid isotopic dilution.

Analytical Procedures. Elemental analyses were performed by Galbraith Laboratories, Knoxville, TN. Infrared spectra were measured from mineral oil (Nujol) mulls between NaCl plates on a Perkin-Elmer 1330 spectrometer and were referenced to the 1028-cm^{-1} band of a 0.05-mm polystyrene film. The solution infrared spectra measured in the carbonyl stretching region were recorded in Beckman F-05 cells equipped with CaF_2 windows. The pathlength was 0.1 mm, and the spectra were referenced to the 1945-cm^{-1} band of a 0.05-mm polystyrene film. ^{17}O NMR spectra were measured on an unlocked FTNMR system equipped with a 5.87-T Oxford Instruments magnet and a Nicolet 1080 data system. The spectra were measured from CH_3CN solutions in 12-mm, vertical sample tubes and were referenced to 25 °C tap water by using the sample replacement method. A preacquisition delay time of 100 μs was utilized for all spectra. Spectra of $[(OC)_3Mn(Nb_2W_4O_{19})][(n\text{-}C_4H_9)_4N]_3$ were recorded without sample spinning using a pulse repetition rate of 5.88 Hz; a spectral bandwidth of 50 000 Hz was digitized from 8192 data points. Spectra of $[(OC)_3Re(Nb_2W_4O_{19})][(n\text{-}C_4H_9)_4N]_3$ were recorded with sample spinning due to the narrow line widths of the OC resonances. The pulse repetition rate was 1.96 Hz; a spectral bandwidth of 32 358 Hz was digitized from 16 384 data points. The pulse width employed for all spectra, 16 μs, corresponded to a 45° pulse. The errors associated with chemical shift values are ±3 ppm for line widths <200 Hz, ±5 ppm for line widths >200 but <400 Hz, and ±7 ppm for line widths >400 Hz. All reported line widths have been corrected for exponential line broadening. The errors associated with line width values are ±20 Hz for line widths <100 Hz, ±40 Hz for line widths >100 but <400 Hz, and ±60 Hz for line widths >400 Hz. Chemical shifts are reported as positive numbers for resonances that are observed at higher frequency (lower field) than the reference.

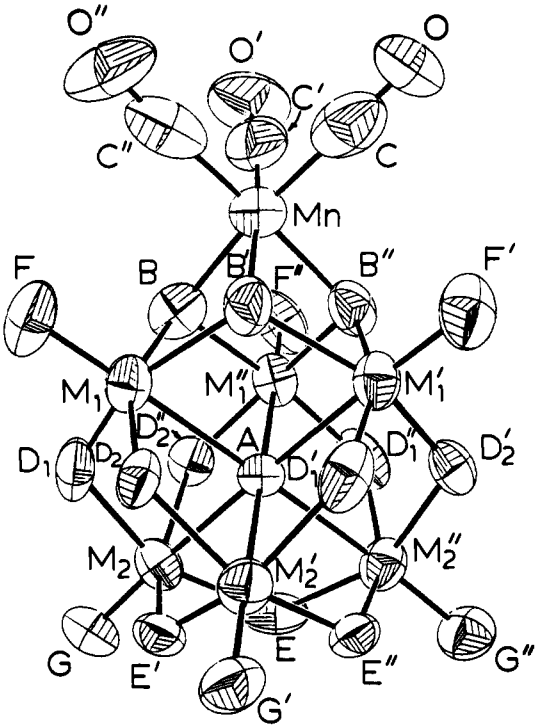

Figure 2. ORTEP model seen in perspective of the anion $[(OC)_3Mn(Nb_2W_4O_{19})]^{3-}$ in crystalline **1**. All atoms are represented by thermal vibration ellipsoids drawn to encompass 50% of the electron density. The disordered niobium/tungsten atom sites in the anion are labeled M_1 and M_2, the manganese atom Mn, and the oxygen atoms by their subscripts according to the following scheme: the unique six-coordinate oxygen O_A; the triply bridging oxygen atoms O_B; the doubly bridging oxygen atoms O_{D_1}, O_{D_2}, and O_E; the terminally bound oxygens O_F and O_G. The carbonyl carbon atoms are labeled C, carbonyl oxygens O. Atoms that are labeled with a single prime or a double prime are related to the unprimed atoms by the crystallographic threefold axis passing through the manganese and O_A atoms.

Preparations. $[(OC)_3Mn(Nb_2W_4O_{19})][(n\text{-}C_4H_9)_4N]_3$. $[(OC)_3Mn(NCCH_3)_3]Br$ was generated in situ by refluxing 0.89 g (3.2 mmol) of $Mn(CO)_5Br$ in 5.8 mL of CH_3CN for 2 h.[17] After the reaction solution was cooled to room temperature and shielded from light, a solution of 7.06 g (3.2 mmol) of $(Nb_2W_4O_{19})[(n\text{-}C_4H_9)_4N]_4$ in 10 mL of CH_3CN was added. The resulting clear, yellow-orange solution was refluxed for 15 min. After it was cooled to room temperature, addition of excess ether (100 mL) caused the product to precipitate as a powdery, yellow solid. The crude product was collected by filtration, washed with 3 × 50 mL ether, and dried in vacuo over P_4O_{10}; yield 6.25 g, 2.99 mmol (93%). Recrystallization was accomplished by dissolving the crude product in excess CH_2Cl_2 (200 mL), adding toluene to the point of near-permanent cloudiness (ca. 50 mL), and then allowing the CH_2Cl_2 to slowly evaporate in the dark. Over a period of 2 days, large block-shaped orange crystals separated from the solution. These were collected by filtration, washed with 3 × 50 mL ether, and air-dried; yield 4.21 g, 2.01 mmol (67%). The analytical sample was recrystallized three times. Anal. Calcd for $C_{51}H_{108}N_3MnNb_2W_4O_{22}$: C, 29.29; H, 5.20; N, 2.01; Mn, 2.63; Nb, 8.88; W, 35.16. Found: C, 29.35; H, 5.22; N, 2.02; Mn, 2.46; Nb, 8.72; W, 34.93. IR: (Nujol, 700–1000 cm^{-1}; see Figure 1b) 747 (s), 767 (sh),

(19) King, R. B. "Organometallic Syntheses"; Academic Press: New York, 1965; Vol. I, p 174.

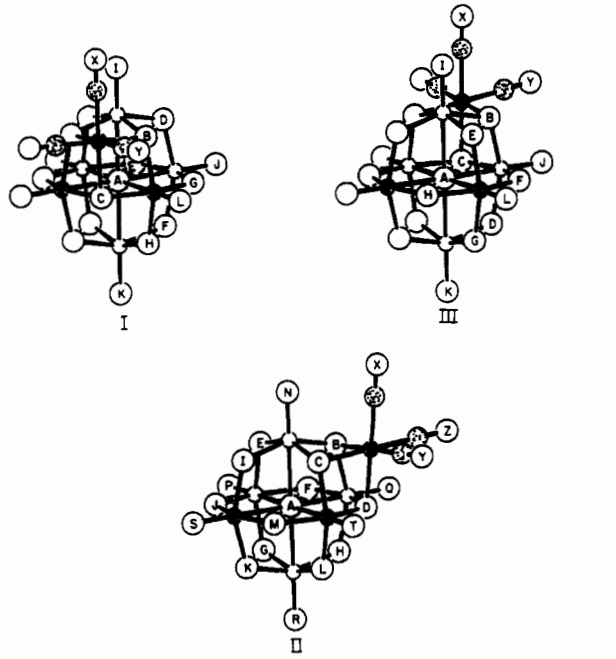

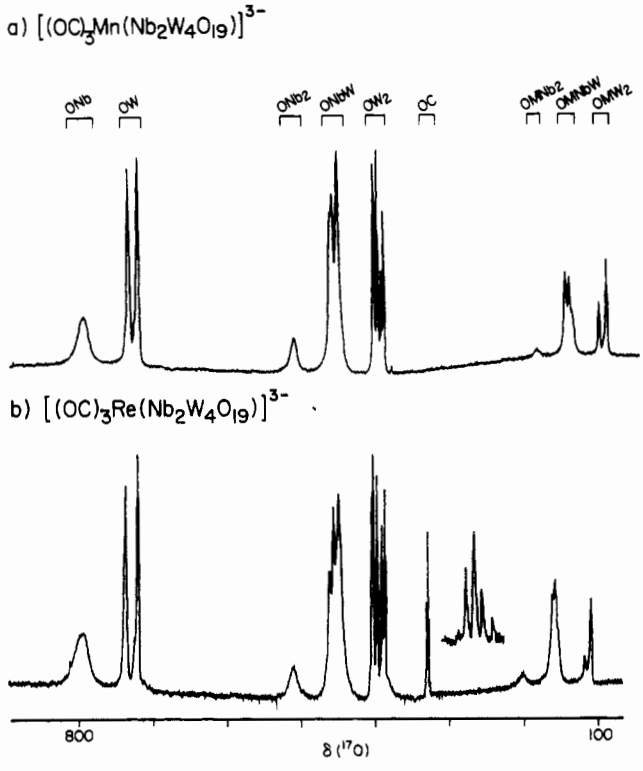

Figure 4. (Top) SCHAKAL drawings of the three $[(OC)_3M(cis\text{-}Nb_2W_4O_{19})]^{3-}$ diastereomers (M = Mn, Re). Within the $Nb_2W_4O_{19}^{4-}$ ligand, the shaded circles represent niobium atoms, the small open circles represent tungsten atoms, and the large open circles represent oxygen atoms. One member of each set of symmetry-equivalent oxygen atoms is labeled. Within the $(OC)_3M$ units, shaded circles represent carbon atoms, open circles represent oxygen atoms, and the filled circles represent M atoms. (Bottom) 33.9-MHz ^{17}O NMR spectra of compounds **1** and **2** measured from 79 °C CH_3CN solutions in (a) and (b), respectively. The inset in (b) is an expansion of the OC region. See Table I for the numerical data and the Experimental Section for spectral parameters. Expansions of the OW_2, $OMNb_2$, OMNbW, and OMW_2 regions of both spectra are shown in Figure 5.

808 (s), 824 (sh), 887 (m), 912 (s), 922 (s), 957 (s), 974 (m) cm^{-1}; (CH_3CN, 1850–2050 cm^{-1}) 1924 (s, br), 2031 (s) cm^{-1}. ^{17}O NMR: (5.3 × 10^{-2} M; 10% ^{17}O; 159 000 acquisitions; 5-Hz exponential line broadening; 79 °C): see Figures 4a and 5a,b and Table I; (5.3 × 10^{-2} M, 10% ^{17}O; 209 000 acquisitions; 27 °C) see Table I.

Table I. 33.9-MHz ^{17}O NMR Chemical Shifts and Line Widths for Compounds 1 and 2[a]

	1		2	
assgnt[b]	27 °C	79 °C	27 °C	79 °C
OMW_2	86 (112) 97 (112)	87 (65) 97 (74)	114 (123) 121 (*c*)	115 (79) 123 (110)
OMNbW	133 137 143 } (428[d])	133 138 143 } (428[d])	159[e] 161 165[e] } (370[d])	159[e] 163 167 } (332[d])
$OMNb_2$	184 (428)	183 (428)	204 (317)	207 (454)
OC			336 (15) 337 (16) 338 (17) 340 (13)	336 (13) 338 (14) 339 (15) 340 (13)
OW_2	394 (70) 398 (*c*) 402 (80) 407 (88)	395 (56) 398 (56) 403 (60) 407 (74) 410[e] (*c*)	396 (86) 401 (*c*) 407 (86) 413 414[e] } (124[d])	398 (48) 400 (*c*) 402 (48) 409 (57) 414 415 416[e] } (92[d])
ONbW	456 463 466 } (442[d])	457 464 466 } (485[d])	460 467 472 } (527[d])	461 468 473 } (576[d])
ONb_2	516 (253)	516 (327)	522 (199)	521 (453)
OW	731 (128) 743 (149)	731 (92) 735[f] (*c*) 743 (114)	737 (142) 754 (172)	736[f] (95) 741[e] (*c*) 751[e] (*c*) 754 755[e] } (124[d]) 758[e] (*c*)
ONb	803 (483)	803 (554)	812 (614)	813 (724)

[a] Chemical shifts are given in ppm followed in parentheses by line widths in Hz, fwhm unless indicated otherwise. The spectra measured at 79 °C are shown in Figures 4 and 5. Information regarding sample preparation, spectral acquisition, and error margins is given in the Experimental Section. [b] M = Mn in **1**, Re in **2**. As discussed in the text, a given oxygen environment is identified by the number and type of atoms an oxygen is bonded to. Resonances for the ONb_2W_4 oxygens in **1** and **2** as well as the OC oxygens in **1** are not observed due to insufficient enrichment. See text for details. [c] Line width could not be measured. [d] Combined line width of bracketed resonances measured at half-maximum of the most intense peak. [e] Shoulder. [f] Chemical shift of band peak, not center of band.

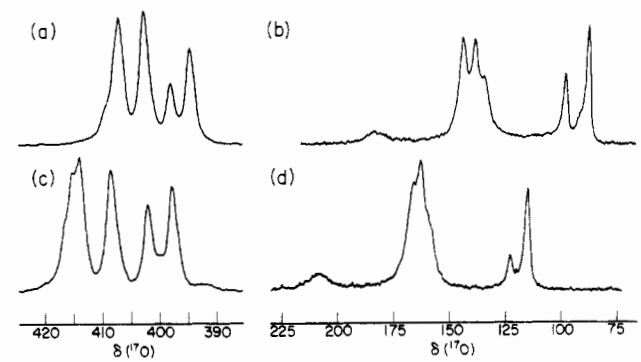

Figure 5. Expansions of the 33.9-MHz ^{17}O NMR spectrum in the δ 390–420 and 75–225 regions: (a and b) compound **1**; (c and d) compound **2**. All of these expansions are derived from the spectra shown in Figure 4 with 10-Hz exponential line broadening.

Solutions of $[(OC)_3Mn(Nb_2W_4O_{19})][(n\text{-}C_4H_9)_4N]_3$ are very light sensitive. During a period of hours in ordinary fluorescent room light, a dark red uncharacterized oil separates from solution. In the solid state, surface discoloration of crystalline product occurs over a period of days.

$[(OC)_3Re(Nb_2W_4O_{19})][(n\text{-}C_4H_9)_4N]_3$. A solution of 0.49 g (0.91 mmol) of $[(OC)_3Re(NCCH_3)_3]PF_6$ in 1.5 mL of CH_3CN was added to

a solution of 2.0 g (0.91 mmol) of $(Nb_2W_4O_{19})[(n\text{-}C_4H_9)_4N]_4$ in 1.5 mL of CH_3CN. The reaction solution was refluxed for 4 h. During this time the solution turned yellow-green in color. After the mixture was cooled to room temperature and then −30 °C, large block-shaped pale yellow crystals of the product separated from the reaction solution. The crystals were collected by filtration, washed with 2 × 3 mL toluene/CH_2Cl_2 (75/25, v/v) and 3 × 10 mL ether, and air-dried; yield 1.23 g, 0.55 mmol (61%). The product at this stage was shown to be pure by IR spectroscopy. Recrystallization was accomplished by cooling hot, saturated CH_3CN solutions to −30 °C. The analytical sample was recrystallized twice. Anal. Calcd for $C_{51}H_{108}N_3ReNb_2W_4O_{22}$: C, 27.56; H, 4.90; N, 1.89; Re, 8.38; Nb, 8.36; W, 33.08. Found: C, 27.60; H, 4.97; N, 1.85; Re, 8.21; Nb, 8.60; W, 32.85. IR: (Nujol, 700–1000 cm^{-1}) 740 (s), 759 (sh), 810 (s), 826 (sh), 884 (m), 918 (s), 928 (s), 960 (s), 978 (m) cm^{-1}; (CH_3CN, 1850–2050 cm^{-1}) 1897 (s, br), 2020 (s) cm^{-1}. ^{17}O NMR: (5.8 × 10^{-2} M; 10% ^{17}O; 79 000 acquisitions; 5-Hz exponential line broadening; 79 °C) see Figures 4b and 5c,d and Table I; (5.8 × 10^{-2} M; 10% ^{17}O; 39 000 acquisitions; 25 °C) see Table I.

X-ray Crystallographic Study[20] of $[(OC)_3Mn(Nb_2W_4O_{19})][(n\text{-}C_4H_9)_4N]_3$ (1). Large well-shaped single crystals of $[(OC)_3Mn(Nb_2W_4O_{19})][(n\text{-}C_4H_9)_4N]_3$ (**1**), obtained by slow (room-temperature) evaporation of $CH_2Cl_2/CH_3C_6H_5$ solution, were suitable for X-ray diffraction studies. The crystals are, at 20 ± 1 °C, trigonal with a = 16.696 (4) Å, α = 64.74 (2)°, V = 3633 (1) Å^3, and Z = 2 (μ_a(Mo K$\bar{\alpha}$)[21a] = 6.96 mm^{-1}; d_{calcd} = 1.912 g cm^{-3}). The systematically absent reflections in the diffraction pattern were consistent with the noncentrosymmetric space group $R3c$-C_{3v}^6 (No. 161)[22a] or the centrosymmetric space group $R\bar{3}c$-D_{3d}^6 (No. 167).[22b] The choice of the noncentrosymmetric space group $R3c$ was indicated by symmetry considerations as well as by the values of various statistical indicators calculated with normalized structure factors; this choice was also fully supported by all stages of the subsequent structure determination and refinement. Both space groups would require some disordering of the Nb and W atoms.

Intensity measurements were made on a Nicolet P$\bar{1}$ autodiffractometer using 1.00° wide ω scans and graphite-monochromated Mo K$\bar{\alpha}$ radiation for a specimen having the shape of a rectangular parallelepiped with dimensions of 0.31 × 0.38 × 0.44 mm. This crystal was glued with epoxy to the end of a thin glass fiber with a tip diameter of 0.20 mm and mounted on a goniometer with its longest dimension nearly parallel to the φ axis of the diffractometer. A total of 2778 independent reflections having $2\theta_{Mo\,K\bar{\alpha}} < 54.9°$ (the equivalent of 1.0 limiting Cu K$\bar{\alpha}$ sphere) were measured in two concentric shells of 2θ containing ~1400 reflections each. A scanning rate of 3°/min was used to measure intensities for reflections having 3.0° < 2θ < 42.9° and a rate of 2°/min for the remaining reflections. The intensity data were corrected empirically for absorption effects using ψ scans for six reflections having 2θ between 8 and 30° (the relative transmission factors ranged from 0.625 to 1.000). The data collection and reduction procedures that were used are described elsewhere;[10] the ratio of total background counting time to net scanning time was 1.00. Averaging Friedel pairs gave 2778 independent reflections having $2\theta_{Mo\,K\bar{\alpha}} < 54.9°$.

The three crystallographically independent metal atoms of **1** were located by using direct methods (MULTAN). Cycles of isotropic unit-weighted full-matrix least-squares refinement for the structural parameters of the three highest peaks found in the E map using W atomic form factors for the two highest peaks and Mn atomic form factors for the third, converged to R_1 (unweighted, based on F)[23] = 0.171 and R_2 (weighted, based on F)[23] = 0.214 for 1212 independent reflections having $2\theta_{Mo\,K\bar{\alpha}} < 42.9°$ and $I > 3\sigma(I)$. The remaining 26 non-hydrogen atoms of the asymmetric unit were located with standard difference Fourier techniques, and their inclusion into the model with isotropic thermal parameters gave R_1 = 0.089 and R_2 = 0.090 for 1212 reflections in cycles of unit-weighted least-squares refinement.

Unit-weighted isotropic full-matrix refinement cycles with the more complete data set and variable occupancies for the two heavier metal sites gave R_1 = 0.101 and R_2 = 0.097 for 2002 independent reflections having $2\theta_{Mo\,K\bar{\alpha}} < 54.9°$ and $I > 3\sigma(I)$. Since the occupancies of both heavier metal sites refined to nearly equal values, which were less than 1.00 (0.92 (1) and 0.95 (1), respectively) when tungsten atomic form factors were used, both metal sites were assumed to be $^1/_3$ Nb and $^2/_3$ W. All subsequent structure factor calculations employed occupancies of 1.00 for these atoms and scattering factors and anomalous dispersion corrections that were $33^1/_3$% Nb and $66^2/_3$% W in character.

Isotropic refinement with mixed form factors and unit occupancies for the disordered metal sites gave R_1 = 0.063 and R_2 = 0.062 for 1212 reflections. Unit-weighted least-squares refinement cycles that utilized anisotropic thermal parameters for all 29 non-hydrogen atoms converged to R_1 = 0.036 and R_2 = 0.035 for 2002 reflections. Hydrogen atoms could not be located from a difference Fourier calculated at this point.

The final cycles of empirically-weighted[24] full-matrix least-squares refinement that utilized anisotropic thermal parameters for all non-hydrogen atoms gave R_1 = 0.036 and R_2 = 0.044 for 2002 independent reflections having $2\theta_{Mo\,K\bar{\alpha}} < 54.9°$ and $I > 3\sigma(I)$. Since a careful comparison of final $|F_o|$ and $|F_c|$ values[20] indicated the absence of extinction effects, extinction corrections were not made.

The correctness of the enantiomeric description was checked using the non-Friedel-averaged data set that contained 4194 reflections, with 2949 of them having $I > 3\sigma(I)$ and $2\theta_{Mo\,K\bar{\alpha}} < 54.9°$. The enantiomer specified by the coordinates in Table II gave R_1 = 0.041 and R_2 = 0.041 for 2949 unit-weighted reflections; the enantiomer with inverted coordinates gave R_1 = 0.043 and R_2 = 0.044.

All structure factor calculations employed recent tabulations of atomic form factors[21b] and anomalous dispersion corrections[21c] to the scattering factors of the W, Nb, and Mn atoms. All calculations were performed

Table II. Atomic Coordinates for Nonhydrogen Atoms in Crystalline $[(OC)_3Mn(cis\text{-}Nb_2W_4O_{19})][(n\text{-}C_4H_9)_4N]_3$[a]

atom type[b]	fractional coord 10^3x	10^3y	10^3z
	Anion		
M_1	391.06 (5)	565.68 (5)	362.16 (5)
M_2	447.80 (5)	418.57 (6)	250.78 (5)
Mn	500[c]	500[c]	500[c]
O_A	406.3 (7)	406.3 (7)	406.3 (7)
O_B	522.5 (6)	502.8 (7)	371.3 (8)
O_{D_1}	429.1 (7)	547.0 (7)	250.8 (7)
O_{D_2}	270.8 (7)	569.2 (6)	386.4 (6)
O_E	452.2 (6)	291.1 (7)	314.5 (8)
O_F	376.5 (7)	678.3 (7)	332.0 (9)
O_G	474.7 (8)	424.3 (8)	137.2 (8)
O	476 (1)	468 (1)	698 (1)
C	481 (2)	483 (2)	623 (2)
	Cation		
N	272 (1)	641 (1)	43 (1)
C_{a_1}	285 (2)	680 (2)	−64 (1)
C_{a_2}	347 (1)	652 (1)	65 (2)
C_{a_3}	175 (1)	705 (2)	84 (2)
C_{a_4}	283 (1)	536 (1)	82 (1)
C_{b_1}	384 (2)	633 (2)	−118 (2)
C_{b_2}	349 (2)	754 (2)	34 (2)
C_{b_3}	145 (2)	671 (2)	188 (2)
C_{b_4}	211 (2)	511 (2)	70 (2)
C_{g_1}	388 (2)	687 (3)	−218 (2)
C_{g_2}	422 (2)	755 (2)	62 (2)
C_{g_3}	77 (3)	731 (2)	226 (2)
C_{g_4}	227 (2)	404 (2)	115 (3)
C_{d_1}	465 (4)	673 (3)	−269 (3)
C_{d_2}	436 (3)	851 (2)	20 (2)
C_{d_3}	36 (2)	719 (2)	330 (2)
C_{d_4}	154 (3)	373 (3)	110 (3)

[a] Numbers in parentheses are the estimated standard deviations in the last significant digit. [b] Atoms are labeled in agreement with Figures 2 and 3.[20] The disordered polyoxoanionic metal atoms are labeled M_1 or M_2 and have $33^1/_3$% Nb and $66^2/_3$% W character. [c] This atom was used to define the origin of the unit cell.

(20) See paragraph at end of paper regarding supplementary material.
(21) "International Tables for X-Ray Crystallography"; Kynoch Press: Birmingham, England, 1974; Vol. IV: (a) pp 55–66; (b) 99–101; (c) 149–50.
(22) "International Tables for X-Ray Crystallography"; Kynoch Press: Birmingham, England, 1969; Vol. I: (a) p 267; (b) p 274.
(23) The R values are defined as $R_1 = \sum||F_o| - |F_c||/\sum|F_o|$ and $R_2 = \{\sum w(|F_o| - |F_c|)^2/\sum w|F_o|^2\}^{1/2}$, where w is the weight given each reflection. The function minimized is $\sum w(|F_o| - K|F_c|)^2$, where K is the scale factor.
(24) Empirical weights were calculated from the equation $\sigma = \sum_0^3 a_n|F_o|^n = 1.85 + (4.49 \times 10^{-3})|F_o| + (1.60 \times 10^{-5})|F_o|^2 + (1.95 \times 10^{-9})|F_o|^3$, the a_n being coefficients derived from the least-squares fitting of the curve $||F_o| - |F_c|| = \sum_0^3 a_n|F_o|^n$, where F_c values were calculated from the fully refined model using unit weighting.

on a Data-General Eclipse S-200 computer equipped with 64K of 16-bit words, a floating-point processor for 32- and 64-bit arithmetic, and versions of the Nicolet EXTL interactive crystallographic software package as modified at Crystalytics Co.

Results and Discussion

Syntheses and Infrared Spectroscopy. Reaction of (*cis*-$Nb_2W_4O_{19}$)[$(n$-$C_4H_9)_4N]_4$ with [*fac*-$(OC)_3M(NCCH_3)_3]X$ (M = Mn^I, X = Br; M = Re^I, X = PF_6) in CH_3CN proceeds according to (1). After the solution is refluxed for 15 min, the M

$$Nb_2W_4O_{19}^{4-} + [(OC)_3M(NCCH_3)_3]^+ \rightarrow [(OC)_3M(Nb_2W_4O_{19})]^{3-} + 3CH_3CN \quad (1)$$

= Mn product can be isolated as a yellow, air-stable, light-sensitive powder by addition of diethyl ether. Formation of the M = Re compound requires a longer reflux period, ca. 4 h, after which the product can be obtained as pale yellow, air-stable crystals by cooling the reaction solution. The products have elemental compositions consistent with the formulations $[(OC)_3M(Nb_2W_4O_{19})][(n\text{-}C_4H_9)_4N]_3$ [M = Mn (**1**), Re (**2**)].

The solution infrared spectra of **1** and **2** in the 1850–2100-cm^{-1} region are characteristic for C_{3v} $M(CO)_3$ units.[25] Their CO stretching frequencies are similar to those for several $(OC)_3ML_3$ complexes where L is a nitrogen donor.[16-18,25] In a typical case, the frequencies for *fac*-$[(OC)_3Mn(propylamine)_3]PF_6$,[16] $\nu_{A_1}(CO)$ = 2032 cm^{-1} and ν_E = 1930 cm^{-1}, closely match those for **1**, 2031 and 1924 cm^{-1}. Comparison of spectra of **1** and **2** with the spectrum of (*cis*-$Nb_2W_4O_{19}$)[$(n$-$C_4H_9)_4N]_4$ in the metal–oxygen stretching region[8] also yields structural information (see Figure 1). In the 850–1000-cm^{-1} terminal oxygen region,[8] the spectra of **1** and **2** have the same pattern of absorptions displayed in the spectrum of $Nb_2W_4O_{19}^{4-}$ but displaced to higher energy by 25–40 cm^{-1}. In the 700–850-cm^{-1} bridging oxygen region,[8] the spectra of **1** and **2** are more complex than the spectrum of $Nb_2W_4O_{19}^{4-}$. Taken as a whole, the comparison suggests that the $M(CO)_3^+$ units in **1** and **2** are bound to bridging oxygens in the *cis*-$Nb_2W_4O_{19}^{4-}$ structure but not to terminal oxygens. This is confirmed by an X-ray diffraction study of **1**, which shows $Mn(CO)_3^+$ bound to three of these bridging oxygens as expected from the 18-electron rule.

Solid-State Structure of $[(OC)_3Mn(Nb_2W_4O_{19})][(n\text{-}C_4H_9)_4N]_3$ (1). The X-ray structural analysis of single crystals of **1** revealed that they are composed of discrete $[(OC)_3Mn(Nb_2W_4O_{19})]^{3-}$ anions (Figure 2) and $(n$-$C_4H_9)_4N^+$ cations (Figure 3).[20] Final atomic coordinates and anisotropic thermal parameters for nonhydrogen atoms are given with estimated standard deviations in Tables II and III,[20] respectively. Bond lengths and angles for the $[(OC)_3Mn(Nb_2W_4O_{19})]^{3-}$ anion and $(n$-$C_4H_9)_4N^+$ cation are given with estimated standard deviations in Tables IV and V,[20] respectively.

The manganese coordination sphere in **1** is unexceptional, having geometric parameters comparable to those of the $(OC)_3MnO_3$ unit in $Mn_3(CO)_8[P(CH_3)_2(C_6H_5)](OC_2H_5)_3$[26] and the $(OC)_3Mn(O/F)_3$ unit in the disordered cubane $Mn_4(CO)_{12}(OH)_{4-x}F_x$.[27] The $Nb_2W_4O_{19}^{4-}$ ligand is bound to the $Mn(CO)_3$ unit by three contiguous bridging oxygen atoms in a fashion also employed by $Nb_6O_{19}^{8-}$ in $[Mn(Nb_6O_{19})_2]^{12-}$,[28] $[(C_5H_5)Ti(Mo_5O_{18})]^{3-}$ in its MoO_2Cl^+ and $Mn(CO)_3^+$ adducts,[4] and $Nb_2W_4O_{19}^{4-}$ in $\{[(CH_3)_5C_5]Rh(Nb_2W_4O_{19})\}^{2-}$.[10]

The most striking feature of the anion structure is the close contact between the carbonyl group carbons and the $Nb_2W_4O_{19}^{4-}$ surface. The average $O_B\cdots C$ distance, 2.89 (3, 9, 9, 2) Å,[29] and the $O_F\cdots C$ distance, 3.26 (3) Å,[29] reflect carbon–oxygen contacts less than or about equal to the van der Waals contact distance, 3.1 Å,[30] apparent in the space-filling representation **b**. Comparison of the complete $[(OC)_3Mn(Nb_2W_4O_{19})]^{3-}$ structure from perspective **c** with the $Nb_2W_4O_{19}^{4-}$ ligand alone, **d**, shows how the three carbonyl groups actually extend the cubic close-packed oxygen framework in a cubic close-packed fashion.

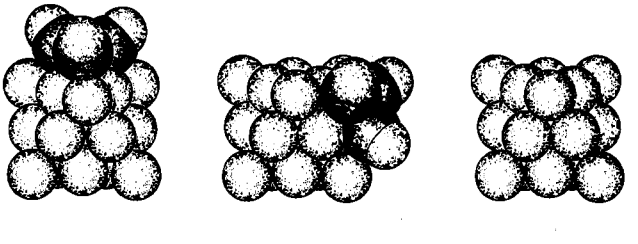

b c d

Note that the environment of the $Mn(CO)_3$ group in $[(OC)_3Mn(Nb_2W_4O_{19})]^{3-}$ is very similar to the $M(CO)_3$ envi-

Table IV. Solid-State Bond Lengths (Å) and Angles (deg) for the $[(OC)_3Mn(cis\text{-}Nb_2W_4O_{19})]^{3-}$ Anion[a,b]

	Distances		
Mn–C	1.843 (27)	M_1–O_A	2.366 (12)
C–O	1.144 (32)	M_2–O_A	2.323 (12)
Mn–O_B	2.001 (12)	M_1–O_F	1.659 (12)
		M_2–O_G	1.721 (11)
M_1–O_B	2.031 (13)		
M_1–O_B'[c]	2.058 (11)	$M_1\cdots M_1'$[c]	3.410 (1)
M_1–O_{D_1}	1.810 (11)	$M_1\cdots M_2$	3.286 (1)
M_1–O_{D_2}	1.851 (12)	$M_1\cdots M_2'$[c]	3.273 (1)
M_2–O_{D_1}	2.031 (11)	$M_2\cdots M_2'$[c]	3.293 (1)
M_2–O_{D_2}''[c]	2.000 (11)		
		Mn···M_1	3.086 (1)
M_2–O_E	1.915 (12)		
M_2–O_E'[c]	1.923 (14)		
	Angles		
MnCO	175 (2)	$M_1O_AM_1'$[c]	92.2 (3)
		$M_1O_AM_2$	89.0 (2)
CMnC'[c]	86 (1)	$M_1O_AM_2'$[c]	88.6 (2)
		$M_2O_AM_2'$[c]	90.3 (3)
$CMnO_B$	173 (1)		
		MnO_BM_1	99.9 (5)
$CMnO_B'$[c]	101 (1)	MnO_BM_1''[c]	99.0 (5)
$CMnO_B''$[c]	94 (1)		
		$M_1O_BM_1''$[c]	113.0 (5)
$O_AM_1O_F$	178.0 (5)	$M_2O_EM_2''$[c]	118.1 (6)
$O_AM_2O_G$	176.9 (5)		
		$M_1O_{D_1}M_2$	117.6 (6)
$M_1O_AM_2''$[c]	178.6 (3)	$M_1O_{D_2}M_2'$[c]	116.4 (5)
$O_FM_1O_B$	104.7 (6)	$O_AM_1O_B$	77.2 (4)
$O_FM_1O_B'$[c]	103.3 (6)	$O_AM_1O_B'$[c]	76.7 (4)
$O_FM_1O_{D_1}$	102.1 (6)	$O_AM_1O_{D_1}$	78.2 (4)
$O_FM_1O_{D_2}$	99.8 (6)	$O_AM_1O_{D_2}$	78.3 (4)
$O_GM_2O_E$	101.9 (6)	$O_AM_2O_E$	75.8 (4)
$O_GM_2O_E'$[c]	102.2 (6)	$O_AM_2O_E'$[c]	75.7 (4)
$O_GM_2O_{D_1}$	107.0 (5)	$O_AM_2O_{D_1}$	75.3 (4)
$O_GM_2O_{D_2}''$[c]	105.6 (5)	$O_AM_2O_{D_2}''$[c]	76.6 (3)

[a] Numbers in parentheses are the estimated standard deviations in the last significant digit. [b] Atoms are labeled in agreement with Figure 2 and Tables II and III.[20] The disordered polyoxoanionic metal atoms are labeled M_1 or M_2 and have 33⅓% Nb and 66⅔% W character. [c] Atoms labeled with a prime are related to those without a prime by the symmetry operation *z*, *x*, *y*; those labeled with double primes are related to those without primes by the operation *y*, *z*, *x*.

(25) Kraihanzel, C. S.; Maples, P. K. *J. Organomet. Chem.* **1976**, *117*, 159–70.
(26) Abel, E. W.; Towle, I. D. H.; Cameron, T. S.; Cordes, R. E. *J. Chem. Soc., Dalton Trans.* **1979**, 1943–9.
(27) Horn, E.; Snow, M. R.; Zeleny, P. C. *Aust. J. Chem.* **1980**, *33*, 1659–65.
(28) Flynn, C. M., Jr.; Stucky, G. D. *Inorg. Chem.* **1969**, *8*, 335–44.

(29) The first number in parentheses following an averaged value of a structural parameter is the root-mean-square estimated standard deviation of an individual datum. The second and third numbers, when given, are the average and maximum deviations from the averaged value, respectively. The fourth number represents the number of individual measurements which are included in the average value.

(30) Pauling, L. "The Nature of the Chemical Bond", 3rd ed.; Cornell University Press: Ithaca, NY, 1960; p 260.

ronment in the cubanes $[(OC)_3M(OR)]_4$ (M = Mn,[31] Re;[32] R = hydrogen, hydrocarbon). As shown in **e**[33] and **f**,[33] where R

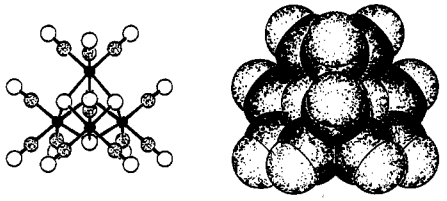

e f

groups have been omitted, each metal tricarbonyl group in these cubanes is bonded to a triangle of oxygen atoms that is in turn surrounded by a larger, approximately copolanar, triangle of CO units. This close-packed layer of three oxygens and three carbonyl groups has precisely the same geometric arrangement formed by the six oxygen atoms that constitute each face of the $Nb_2W_4O_{19}^{4-}$ ion. Comparison of **b** with **f** shows this analogy quite clearly. This structural analogy exists because the $[(OC)_3M(Nb_2W_4O_{19})]^{3-}$ structure itself contains a cubane subunit evident from comparison of the cubane structure, **g**, [33] and the hexametalate adduct

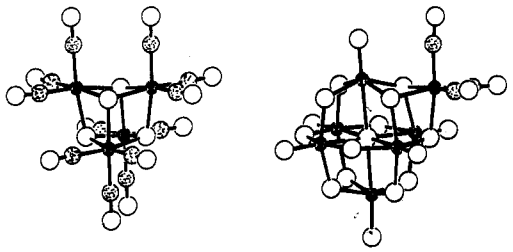

g h

structure, **h**, viewed from the same perspective. Referring to Figure 2, the interpenetrating tetrahedra that form the core of the cubane subunit in the hexametalate adduct structure are defined by Mn, M_1, M_1', and M_1'' and O_A, O_B, O_B', O_B''.

The six (M_1 and M_2) polyoxoanion framework metal atoms appear to be statistically disordered in the solid state, with each possessing 33% Nb and 66% W character. Given the presence of a *cis*-$Nb_2W_4O_{19}^{4-}$ anion, such disorder is consistent with the presence of one or more diastereomeric metal tricarbonyl adducts (see Figure 4a). Specifically, three possibilities must be considered: (a) racemic diastereomer II; (b) equal amounts of diastereomers I and III; (c) a combination of (a) and (b). Unfortunately, the X-ray diffraction data could not be used to distinguish between these possibilities, and an ^{17}O NMR study described below was performed to resolve this ambiguity.

Although the crystallographic data do not permit a determination of isomeric composition for anion **1**, it does allow qualitative structural characterization of the interaction of a $Mn(CO)_3^+$ cation with the *cis*-$Nb_2W_4O_{19}^{4-}$ anion. Since the nature of this interaction is similar to but more significant than that of the $[(CH_3)_5C_5]Rh^{2+}$ cation with the *cis*-$Nb_2W_4O_{19}^{4-}$ anion, the reader is referred to ref 10 for a detailed discussion. Two principal effects are to be noted. First, cation binding induces a sequence of trans bond length alternations at bridging oxygens in the $Nb_2W_4O_{19}^{4-}$ ligand (see Table IV): $d_{O_B-M_1}$ = 2.045 (12, 14, 14, 2) Å,[29] $d_{M_1-O_D}$ = 1.831 (12, 21, 21, 2) Å, $d_{O_D-M_2}$ = 2.016 (11, 16, 16, 2) Å, $d_{M_2-O_E}$ = 1.919 (13, 4, 4, 2) Å. Second, cation binding significantly displaces the approximately coplanar layers of atoms in the $Nb_2W_4O_{19}^{4-}$ ligand relative to each other, producing the interlayer separations shown in Chart I.[34]

Chart I

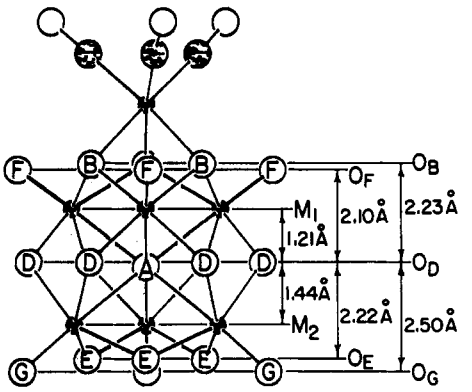

^{17}O NMR Spectroscopy. Oxygen-17 NMR spectra of compounds **1** and **2** are shown in Figures 4 and 5; chemical shift data are presented in Table I. Assignments made in Figure 4 and Table I are made according to the number and identity of the atoms to which a given type of oxygen is bonded. These assignments were made by comparison with chemical shifts for oxygens having similar environments in related polyoxoanions[3,4,10,15,35] and metal carbonyls.[36]

All ^{17}O NMR spectra were measured from samples of **1** and **2** enriched in ^{17}O, and this enrichment was selective in at least two respects. First, the carbonyl oxygens were ^{17}O enriched in **2**, but not in **1**. Both **1** and **2** were prepared from ^{17}O-enriched $Nb_2W_4O_{19}^{4-}$ plus unenriched $(OC)_3M(NCCH_3)_3^+$ according to eq 1. Since oxygens in the $Nb_2W_4O_{19}^{4-}$ anion bonded to niobium exchange with water oxygens rapidly[10] and since manganese and rhenium carbonyls can undergo facile oxygen exchange with water,[37] traces of water may be acting as the transfer agent. Direct transfer cannot, however, be ruled out. The failure to observe CO enrichment in **1** may simply reflect the short reaction time. A second type of selective enrichment arises during the enrichment of $Nb_2W_4O_{19}^{4-}$ by exchange with $^{17}OH_2$ as described in ref 10. This procedure gives very little ^{17}O enrichment at the central ONb_2W_4 oxygen, and there is some evidence that enrichment at the unique OW_2 oxygen is also low.[10] Resonances for O_A in diastereomers I–III (see Figure 4) are therefore not observed, and it is possible that resonances for O_E in I, O_F in II, and O_C in III are not observed or are observed with reduced intensity. All other $Nb_2W_4O_{19}^{4-}$ oxygens in I–III are enriched to the same extent, however.[10]

Analysis of the spectra of **1** and **2** shown in Figures 4 and 5 in the $OMNb_2$, OMNbW, and OMW_2 regions provides conclusive evidence for the presence of all three $[(OC)_3M(Nb_2W_4O_{19})]^{3-}$ diastereomers. Observation of an $OMNb_2$ resonance establishes the existence of diastereomer I since only this isomer contains an oxygen of this type, O_C. Three resonances are observed in the OMNbW region, two having approximately equal intensity plus a less intense shoulder. Since isomer III contains no OMNbW oxygens, isomer II contains two nonequivalent OMNbW oxygens (O_C and O_D) and isomer I contains two equivalent OMNbW oxygens (O_B), the two intense OMNbW resonances arise from

(31) Abel, E. W.; Farroe, G.; Towle, I. D. H. *J. Chem. Soc., Dalton Trans.* **1979**, 71–3.
(32) Herberhold, M.; Suess, G.; Ellerman, J.; Gäbelein, H. *Chem. Ber.* **1978**, *111*, 2931–41.
(33) Coordinates for these drawings are taken from ref 27.
(34) The reference plane used in Chart I is defined by the six O_D atoms in **1**. The least-squares mean plane through the six atoms, which are coplanar to within 0.004 Å, is defined by $0.3660x + 0.4983y + 0.7860z = 16.096$, where x, y, and z are orthogonal coordinates measured in angstroms along $(\vec{b} \times \vec{c}^*)$, $\vec{b}$, and $\vec{c}^*$, respectively, of the unit cell. The O_B, O_F, M_1, M_2, O_E, and O_G atoms in **1** are displaced from this reference plane by 2.230 (11), 2.102 (11), 1.211 (1), 1.436 (1), 2.215 (12), and 2.500 (11) Å, respectively.
(35) Filowitz, M.; Ho, R. K. C.; Klemperer, W. G.; Shum, W. *Inorg. Chem.* **1979**, *18*, 93–103.
(36) Hickey, J. P.; Wilkinson, J. R.; Todd, L. J. *J. Organomet. Chem.* **1979**, *179*, 159–68.
(37) Darensbourg, D. J.; Froelich, J. A. *J. Am. Chem. Soc.* **1977**, *99*, 5940–6 and references cited therein.

isomer II and the shoulder arises from isomer I. The OMW_2 region contains two resonances. Since diastereomer I contains no OMW_2 oxygens and diastereomer II contains a single OMW_2 oxygen, O_B, diastereomer III must be present. The more intense OMW_2 resonance has about the same intensity as the two more intense OMNbW resonance and is therefore assigned to O_B in isomer II. The less intense resonance arises from diastereomer III.

Although the relative intensities of the resonance just discussed reflect the relative abundances of diastereomers I–III, the range of line widths present and overlapping nature of several resonances make a truly quantitative assessment of the isomer distribution impossible. A qualitative view is obtained easily, however. The ratio of the $OMNb_2$ resonance's intensity to the intensity of either of the more intense OMNbW resonances directly reflects the relative concentrations of diastereomers I and II, and II is clearly predominant. The ratio of the less intense OMW_2 resonance's intensity to the intensity of either of the more intense OMNbW resonances divided by 2 sets an upper limit on the ratio of isomer III concentration to isomer II concentration, and isomer II clearly predominates here also. The situation is complicated by the fact that the less intense OMW_2 resonance arises from the two O_B oxygens in isomer III and possibly the O_C oxygen in isomer III, depending upon the level of ^{17}O enrichment at this O_C site (see above). Since purely statistical factors favor the C_1 symmetry diastereomer II over the C_s diastereomers I and III by a factor of 2, the observed I:II:III isomer distribution approximates the 1:2:1 statistically random situation.

Acknowledgment. W.G.K. acknowledges the National Science Foundation for partial support of this research. NMR experiments were conducted with assistance from D. Warrenfeltz at the University of Illinois NSF Regional NMR Facility (Grant CHE97-16100). We are grateful to Dr. Egbert Keller for providing a copy of his SCHAKAL program and to S. Moenter for providing SCHAKAL drawings.

Registry No. **1** (isomer I), 93530-16-6; **1** (isomer II), 93530-21-3; **1** (isomer III), 93564-54-6; **2** (isomer I), 93530-18-8; **2** (isomer II), 93530-23-5; **2** (isomer III), 93530-25-7; $[(OC)_3Mn(NCCH_3)_3]Br$, 93530-19-9; $(Nb_2W_4O_{19})[(n\text{-}C_4H_9)_4N]_4$, 60098-33-1; $[(OC)_3Re(NCCH_3)_3]PF_6$, 66610-18-2.

Supplementary Material Available: Crystal structure analysis report, Tables III (anisotropic thermal parameters for non-hydrogen atoms) and V (cation bond lengths and angles), Figure 3 (ORTEP drawing of the cation), and structure factor tables for the X-ray structural study of $[(OC)_3Mn(Nb_2W_4O_{19})][(n\text{-}C_4H_9)_4N]_3$ (19 pages). Ordering information is given on any current masthead page.

Contribution from the Department of Chemistry,
Dalhousie University, Halifax, Nova Scotia, B3H 4J3 Canada

Synthesis of $[Rh_2(\mu\text{-}OR)(CO)_2(\mu\text{-}PPh_2CH_2PPh_2)_2]ClO_4$ (R = H, CH_3, C_2H_5) and Their Use as Synthetic Precursors to Other A-Frame Complexes

SAMITHA P. DERANIYAGALA and KEVIN R. GRUNDY*

Received July 29, 1983

General preparative methods for the synthesis of a variety of A-frame complexes, $[Rh_2(\mu\text{-}X)(CO)_2(\mu\text{-}dppm)_2]^+$, are presented, including examples in which the bridgehead ligand X has an oxygen or nitrogen donor atom. The reaction of *trans*-$[Rh_2Cl_2(CO)_2(\mu\text{-}dppm)_2]$ with excess RO^- and $NaClO_4$ in the appropriate alcohol suspension yields $[Rh_2(\mu\text{-}OR)(CO)_2(\mu\text{-}dppm)_2]ClO_4$ (R = Me, Et). Recrystallizing the alkoxide complexes in the presence of excess $HClO_4$ gives $[Rh_2(\mu\text{-}OH)(CO)_2(\mu\text{-}dppm)_2]ClO_4$. A similar hydroxide complex $[Rh_2(\mu\text{-}OHCl)(CO)_2(\mu\text{-}dppm)_2]\cdot H_2O$ results from the reaction of *trans*-$[Rh_2Cl_2(CO)_2(\mu\text{-}dppm)_2]$ with Na_2CO_3 in aqueous ethanol. The bridging ligands in $[Rh_2(\mu\text{-}OR)(CO)_2(\mu\text{-}dppm)_2]ClO_4$ (R = H, Me, Et) are acid labile, enabling a range of substitution reactions to be performed. Thus, complexes of the type $[Rh_2(\mu\text{-}X)(CO)_2(\mu\text{-}dppm)_2]ClO_4$ with X = Cl, Br, I, O_2CH, O_2CCH_3, O_2CCF_3, NCO, and N_3 can be synthesized. The trifluoroacetate group in $[Rh_2(\mu\text{-}O_2CCF_3)(CO)_2(\mu\text{-}dppm)_2]ClO_4$ is also labile, making this compound a useful synthon. With excess MX, complexes of the type $[Rh_2(\mu\text{-}N_3)(CO)_2(\mu\text{-}dppm)_2]ClO_4$ and $[RhX(CO)(dppm)]_2$ (X = NCO, NCS) can be isolated. With 1 equiv of NH_4NCS, $[Rh_2(\mu\text{-}O_2CCF_3)(CO)_2(\mu\text{-}dppm)_2]ClO_4$ yields $[Rh_2(\mu\text{-}NCS)(CO)_2(\mu\text{-}dppm)_2]ClO_4$. The N-bound isomer is also obtained when $[Rh_2(\mu\text{-}OEt)(CO)_2(\mu\text{-}dppm)_2]ClO_4$ reacts with NH_4NCS in the presence of $HClO_4$, but when the acid is omitted, the S-bound isomer $[Rh_2(SCN)(CO)_2(\mu\text{-}dppm)_2]ClO_4$ results.

Introduction

Recently, the chemistry of the rhodium A-frame complexes, typified by $[Rh_2(\mu\text{-}Cl)(CO)_2(\mu\text{-}dppm)_2]^+$,[1] $Rh_2(\mu\text{-}CO)Cl_2(\mu\text{-}dppm)_2$,[2] and $Rh_2(\mu\text{-}S)(CO)_2(\mu\text{-}dppm)_2$,[3] has attracted considerable attention, especially with respect to the ability of these compounds to coordinate small molecules such as carbon monoxide, sulfur dioxide, and acetylenes in a bridging fashion. This phenomenon has obvious relevance to catalytic processes occurring either on transition-metal clusters or on metal surfaces, and in fact, a number of A-frame complexes are capable of homogeneous hydrogenation,[1,4] hydroformylation, and catalysis of the water gas shift reaction.[4] Despite this, however, the relationship between catalytic activity and binding of the substrate in the bridging position has not been established.

In the chemistry of the rhodium A-frame complexes so far investigated, the principal function of the bridgehead ligand has been to link the two rhodium-containing square planes, thereby orienting the metal centers in the appropriate fashion. In addition, it is obvious that the bridging ligand has a profound effect upon the ability of the A-frame complex to coordinate small molecules in the endo pocket. Our work with A-frame complexes stems from a long-term interest in ligand reactivity. Since it seems natural to expect that certain bridging ligands should have an interesting

(1) Mague, J. T.; Sanger, A. R. *Inorg. Chem.* **1979**, *18*, 2060.
(2) Cowie, M.; Dwight, S. K. *Inorg. Chem.* **1980**, *19*, 2500.
(3) Kubiak, C. P.; Eisenberg, R. *Inorg. Chem.* **1980**, *19*, 2726.
(4) Kubiak, C. P.; Woodcock, C.; Eisenberg, R. *Inorg. Chem.* **1982**, *21*, 2119.

0020-1669/85/1324-0050$01.50/0